scientific reports

Check for updates

OPEN

GOLPH3 promotes calcium oxalate-induced renal injury and fibrosis through Golgi stress-mediated apoptosis and inflammatory responses

Bao-feng Song[1,2], Bo-jun Li[1,2], Yushi Sun[1,2], Ming Li[1], Ting Rao[1]✉, Yuan Ruan[1]✉ & Fan Cheng[1]✉

A common urological disorder, calcium oxalate (CaOx) stones are the most common form of kidney stones. Deposition of CaOx crystals leads to tubular damage, interstitial fibrosis, and chronic kidney disease. Understanding the intrinsic mechanisms of kidney stone formation is essential for the prevention of kidney stones and the development of new therapeutic agents. The Golgi apparatus is a key organelle in the secretory pathway of eukaryotic cells, which plays an important role in the sorting, modification, and transport of proteins within the cell, and has been reported to be involved in several diseases, including prostate tumors, gastrointestinal tumors, sepsis, and so on. GOLPH3 is also known as GPP34, GMx33, or MIDAS. It is a glycoprotein that regulates traffic between the trans-Golgi network and the cell membrane. However, its role in renal injury caused by CaOx crystal deposition is still unclear. Results from immunohistochemistry, qRT-PCR, western blot, and public database single nucleotide RNA-seq showed that GOLPH3 was significantly upregulated in kidney stone patients and animal kidneys. Significant inhibition of Golgi stress, apoptosis, and renal fibrosis by GOLPH3 inhibition with siRNA in CaOx-stimulated HK-2 cells. The PI3K\AKT\mTOR signaling pathway was inhibited by GOLPH3 knockdown, which may be associated with reduced inflammatory response and apoptosis, as well as restoration of Golgi morphology and function. In conclusion, GOLPH3 plays a critical role in CaOx-induced kidney injury by promoting Golgi stress and increasing inflammatory responses, apoptosis, and renal fibrosis, suggesting that GOLPH3 is a potential therapeutic target for kidney stones.

Keywords Kidney stones, CaOx, GOLPH3, Golgi

Kidney stones, being one of the most prevalent urinary system disorders, place a significant financial and medical burden on both patients and the community[1]. Epidemiological surveys have revealed a global rise in the incidence of kidney stones, with recurrence rates reaching as high as 50% within 5 years[2,3]. Due to the high recurrence rate, kidney stones are now recognized as a chronic systemic disease[4]. The prolonged presence of kidney stones can result in fluid retention within the kidneys and, in severe cases, may even lead to impaired kidney function or complete renal failure. Calcium oxalate is the predominant constituent of renal stones, constituting approximately 70% of all kidney stones. Multiple mechanisms leading to kidney injury induced by Calcium oxalate have been demonstrated, including inflammatory injury, oxidative stress, and macrophage polarization[5–7]. However, currently, there is no established method to prevent the formation of kidney stones or to reduce their occurrence and recurrence. Therefore, it is imperative to approach the mechanism of kidney stone formation from a fresh perspective and investigate the causes and treatments of stones to effectively prevent their reoccurrence.

The Golgi apparatus is a vital organelle involved in intracellular transport, responsible for the secretion of lipids and proteins to their designated locations within the cytosol[8–10]. Moreover, recent studies have demonstrated

[1]Department of Urology, Renmin Hospital of Wuhan University, Wuhan 430060, China. [2]Bao-feng Song, Bo-jun Li and Yushi Sun contributed equally to this work. ✉email: tinart@126.com; 10733638@qq.com; urology1969@aliyun.com

that the Golgi apparatus can function as a sensor and a central effector in the cellular death pathway, responding to various stress signals[11,12]. The disruption of Golgi structure and functions, known as Golgi stress, triggers Golgi disassembly and fragmentation and has been reported in various diseases including many inflammatory diseases and tumors[13–16]. Golgi phosphoprotein 3 (GOLPH3) is located on the Golgi membrane and has been reported to regulate Golgi transport[17]. GOLPH3 directly interacts with phosphatidylinositol 4-phosphate (PtdIns4P) and tightly binds to unconventional myosin 18A (MYO18A)[18,19]. This interaction generates the necessary tension for vesicle outgrowth, paracrine transport, and the maintenance of Golgi morphology. GOLPH3 has been identified as a novel oncogene protein that plays a crucial role in cell proliferation and tumor progression pathways. The GOLPH3 gene is amplified in various solid tumors, including prostate, gastric, and liver cancers[20–23]. Importantly, there is evidence indicating that GOLPH3 overexpression activates the PI3K/AKT/mTOR pathway, which is involved in proliferation, differentiation, apoptosis, and microangiogenesis in different types of tumor cells[8,24–26].

Recent studies have demonstrated that GOLPH3 is upregulated in endotoxemia-induced lung injury, liver injury, and acute kidney injury. Moreover, it has been suggested that GOLPH3 might serve as a sensor of Golgi stress during cellular damage and transmit stress signals to downstream effectors, thereby altering cellular function[27]. However, the roles and mechanisms of Golgi stress and GOLPH3 in renal stone formation have not been extensively studied. Therefore, we conducted ex vivo experiments to investigate the role of GOLPH3 in a calcium oxalate-induced renal stone model.

Materials and methods

Clinical specimens

All samples were obtained from the Department of Urology, People's Hospital of Wuhan University, China. Tissue samples for the kidney stone group (KS, n = 6) were taken from patients with non-functioning kidneys due to CaOx kidney stones. Tissue samples for the normal control group (NC, n = 6) were obtained from adjacent non-tumor kidney tissues from patients who underwent radical nephrectomy. This study was approved by the Ethics Committee of Wuhan University People's Hospital (approval number: WDRY2021-KS047).

Animal models and protocols

Wild-type male C57BL/6J mice (6–8 weeks, weighing 24-28 g) were purchased from Hubei Provincial Centers for Disease Control and Prevention (Wuhan, China) and maintained in the animal facility at Renmin Hospital of Wuhan University. All animal treatments were approved by the Laboratory Animal Welfare and Ethics Committee of the Renmin Hospital of Wuhan University (approval number: WDRM-20200604), and performed by the National Institute of Health (NIH) guidelines for laboratory animal care. The mice were kept under specific pathogen-free conditions and in a steady temperature (22 ± 2 °C) and humidity (40–70%) barrier system with a 12-h light/dark cycle, with food and water available.

Twelve male mice were randomly divided into two groups: the control group and the hyperoxaluric mouse model group. The control group received intraperitoneal injections of saline, while the hyperoxaluric group received glyoxylate injections (120 mg/kg/d) from days 0 to 10. On the tenth day, all mice were euthanized, and blood samples were collected from the heart. The blood was centrifuged at 3000×*g* for 15 min to obtain plasma, which was then stored at − 80 °C for further biochemical analysis. Kidneys were collected and either snap-frozen in liquid nitrogen at − 80 °C for storage or fixed in 10% buffered formalin for subsequent analysis. All methods are reported in accordance with ARRIVE guidelines. All procedures were done according to the protocols approved by the Clinical Research Ethics Committees of Renmin Hospital of Wuhan University and conducted according to the guidelines of ethical management. Committee approval number: WDRM20200604.

Cell culture and treatment

The human proximal tubular epithelial cells (HK-2) were obtained from the Cell Bank of the Chinese Academy of Sciences (Shanghai, China). These cells were cultured in MEM supplemented with 10% fetal bovine serum (Gibco, Waltham, MA, United States), 1% penicillin, and streptomycin. The cell culture was maintained at a temperature of 37 °C with 5% CO2 in a humidified environment. HK-2 cells were stimulated with COM (calcium oxalate monohydrate) at a concentration of 200 μg/ml to mimic the in vitro environment of kidney stones.

GOLPH3 siRNA was used to reduce the GOLPH3 expression. HK-2 cells in the growth phase were seeded in six-well plates at a density of 2×10^5 cells per plate and incubated for 24 h. GOLPH3-specific small interfering RNA (siRNA) and corresponding control siRNA were obtained from GenePharma (Shanghai, China). HK-2 cells were carried out by using lipofectamine 2000 (Invitrogen, MA, USA) according to the manufacturer's instructions. The cells were transfected with GOLPH3-specific siRNA using the instructions provided by the reagent supplier. The efficiency of siRNA-mediated inhibition was confirmed by Western blotting.

Immunohistochemistry

After fixation with 4% paraformaldehyde and embedding in paraffin, the tissues were sectioned into 4-μm thick slices. These sections were then incubated overnight at 4 °C with anti-GOLPH3 antibody (1:500; Proteintech, Wuhan, China), followed by incubation with horseradish peroxidase (HRP)-conjugated goat secondary antibody at 37 °C for 1 h. The following day, the sections were visualized using 3,3′-diaminobenzidine (DAB). The positive signals in the kidneys were quantified under a microscope in 10 non-repetitive fields of view (× 200 magnification).

Terminal deoxynucleotidyl transferase dUTP nick-end labeling(TUNEL) assay

Paraffin-embedded renal slices were examined with a Colorimetric TUNEL Apoptosis Staining Kit (Beyotime Biotechnology, China) to detect apoptotic cells, and the nuclei were counterstained with DAPI. Before staining,

cells were fixed in 4% paraformaldehyde and 0.1% Triton X-100. The TUNEL-positive cells were counted using ImageJ software.

Real-time quantitative polymerase chain reaction

Total RNA was extracted using TRIzol reagent (Invitrogen Life Technologies), followed by reverse transcription to obtain cDNA. Real-time quantitative polymerase chain reaction (qPCR) amplification was performed using SYBR Green Master Mix (Yeasen, Shanghai, China) according to the manufacturer's instructions. Amplification was performed for 45 cycles consisting of 5 s at 95 °C, and 30 s at 72 °C, then 30 s at 64 °C. The relative mRNA expression of each gene was normalized to the expression level of the gene GAPDH. The primer sequences are listed in Table 1.

Kidney precision medicine project

The Kidney Precision Medicine Project (KPMP) is a project funded by the NIDDK with the purpose of understanding and finding new ways to treat chronic kidney disease (CKD) and acute kidney injury (AKI). It contains a reference atlas of a healthy and diseased kidney using datasets from kidney biopsies and reference tissue samples analyzed with transcriptomics, proteomics, metabolomics, and spatial omics approaches. In this study, the Kidney Tissue Atlas Explorer was used (https://atlas.kpmp.org/explorer/) to access GOLPH3 expression in renal tubular epithelial cells obtained with single-cell RNA sequencing. (Data Coverage: N = 47 participants, 20 health reference (HRT), 15 with chronic kidney disease, 12 with AKI).

Western blot analysis

Kidney tissues or cells were lysed with RIPA lysis buffer (Servicebio, China) containing phenylmethylsulfonyl fluoride (PMSF) and phosphatase inhibitor cocktail, and tissue and cell lysates were prepared by sonication 3 times for 5 min each. Total protein concentration was quantified in the lysates using a bicinchoninic acid (BCA) assay kit (Beyotime Biotechnology, China). Proteins were separated using the sodium dodecyl-sulfate polyacrylamide gel electrophoresis (SDS-PAGE) method and then transferred to a PVDF membrane, which was closed with 5% skimmed milk for 1 h at 25 °C. The membrane was then blocked with 5% skimmed milk for 1 h at 25 °C. The PVDF membranes were incubated for 12 h at 4 °C with the following primary antibodies: anti-GOLPH3(ab236296,rabbit,1:1000), anti-GRASP65 (Golgi peripheral membrane protein p6510747-2-AP,rabbit,1:5000, Protenintech), anti- ARF4 (ADP-ribosylation factor 4, ab171746, rabbit, 1:10,000), anti-PI4KIIIβ (phosphatidylinositol 4-kinase III beta, ab134756, rabbit, 1:10,000), anti-MYO18A (14611-1-AP,

Genes	Primer sequence (5′–3′)
	F: CTAGAGGCTTGTGGAATGAGACG
GOLPH3(Homo)	
	R: GACCGTTTCTGGAGGCTGAGTT
	F: ACAAGGGCGACTCCAAGGA
GOLPH3(Mus)	
	R: ATGATGTGTAACCCTCTCGGT
	F: TAGTTGGCTCTGACCAGATTCT
Grasp65(Mus)	
	R: CCATAACCAATACCACACCCC
	F: CTGGCAAGACGACAATTCTGT
ARF4(Mus)	
	R: TGGATTCTTTCACGATCATTGCT
	F: ATGGGAGACATGGTAGTGGAG
PI4KIIIβ(Mus)	
	R: TGACGCTTAGTAGGGAGCCC
	F: TGACAGCAATCGGGGTAGC
MYO18A(Mus)	
	R:GGCTCCGTTGAGAGAAGGAA
	F: ACTACTGCCGAGCGTGAGAT
α-SMA(Mus)	
	R: AGGTAGACAGCGAAGCCA
	F: GCTCCTCTTAGGGGCCACT
Collagen-I(Mus)	
	R: ATTGGGGACCCTTAGGCCAT
	F: CGTCCACACGCACCTACAG
Vimentin(Mus)	
	R: GGGGGATGAGGAATAGAGGCT

Table 1. RT–PCR primer sequences.

rabbit, 1:6000, Protenintech), anti-α-SMA (GB111364; 42 kDa, 1:1000, Servicebio), anti-vimentin (ab217673, rabbit, 1:1000), anti-CollagenI (ab138492, rabbit, 1:1000), anti-AKT (ab38449, rabbit, 1:1000), anti-p-AKT (ab8805, rabbit, 1:1000), anti-PI3K (ab302958, rabbit, 1:1000), anti-p-PI3K (ab182651, rabbit, 1:500), anti-Mtor (ab109268, rabbit, 1:2000), anti-p-mTOR (67778-1-Ig, mouse, 1:10,000, Protenintech), anti-β-actin (81,115–1-RR, rabbit, 1:5000, Protenintech). After washing the membranes, the membranes were incubated with horseradish peroxidase (HRP)-conjugated secondary antibody for 1 h at 25 °C and washed again. The membranes were washed with TBST for 10 min each time. Target bands were visualized using Omni-ECL™Femto Light Chemiluminescence Kit (Epizyme Biotech, China) on a ChemiDoc MP system (Bio-Rad, USA).

Immunofluorescence

For kidney tissue sections and cell crawls that had been fixed with 4% paraformaldehyde were incubated with 0.1% Triton X-100 for 20 min then blocked with 5% goat serum, then cells and tissues were incubated with primary antibodies for 12 h at 4 °C, washed, followed by staining with CY3- or Alexa Fluor-488-conjugated secondary antibodies (1:1000; Thermo Scientific, MA, USA). The slides were mounted for examination after being stained with 4′,6-diamidino-2-phenylindole. Using the same settings on a fluorescence microscope (Nikon).

Renal function analysis

Blood urea nitrogen (BUN) and serum creatinine (Scr) levels were measured according to the instructions of the kit (Beyotime Biotechnology, Shanghai, China).

ELISA

IL-1β, TNF-α, and IL-6 levels were tested using ELISA kits (Beyotime Biotechnology, China) according to the manufacturer's instructions.

Flow cytometry

Apoptosis analysis was assessed by flow cytometry according to standard protocols. Cells were seeded into 6-well plates in which the modeling group was treated by adding 200 μg/ml of COM for 24 h. Cells were harvested at a density of 1×10^6 cells/well. After rinsing twice with PBS, apoptosis was detected by flow cytometry (CytoFLEX, Beckman, Coulter) using the Annexin V-FITC/PI Apoptosis Detection Kit (Beyotime Biotechnology, China). Data were analyzed with FlowJo 10.6.2 software.

Kidney histopathological examination

Paraffin-embedded renal tissues were cut into 4-μm-thick sections, rehydrated and stained with hematoxylin–eosin (HE), and the tubular damage score was used to assess tissue damage, with HE sections scored on a 0–4 scale of 0, normal; 1, mild (< 25% tubular damage); 2, moderate (25–49% tubular damage); 3, severe (50–75% tubular damage); 4, extensive damage (> 75% tubular damage). Collagen fiber deposition was detected using Sirius Red and Masson staining, and the percentage of collagen deposition area in kidney sections was quantified using ImageJ software (1.8.0). Kidney sections were stained for crystal deposition using von Kossa histologic staining. Quantification of renal crystals on von Kossa stained tissue sections using ImageJ software.

Statistical analyses

Data analysis was done by GraphPad Prism software (version 8.0; GraphPad Software, CA, USA). Experiment results are shown as means standard deviation. Examining group differences involved using the Student's t-test and one-way analysis of variance. $P < 0.05$ was considered statistically significant.

Ethics statement

All procedures were done according to the protocols approved by the Clinical Research Ethics Committees of Renmin Hospital of Wuhan University and conducted according to the guidelines of ethical management.

Consent to publish

All patients signed informed consent to publish their data.

Results

Up-regulation of GOLPH3 expression in renal tissues of patients with kidney stones

To confirm the damage of kidney stones to human kidneys, renal tubular epithelial apoptosis was detected by tunel in patients with kidney stones, and increased apoptosis of renal tubular epithelial cells in patients with kidney stones can be seen in Fig. 1A. Further detection of the expression of GOLPH3 in kidney stone patients, we examined GOLPH3 expression in NC and KS, as shown in Fig. 1B, GOLPH3 expression was up-regulated in the kidneys of kidney stone patients compared to controls, Western blot and qPCR (Fig. 1E, C) showed the same results. Single-nucleus RNA-seq (SNRNA-seq) showed that GOLPH3 was up-regulated in the nucleus of proximal renal tubular epithelial cells during AKI and CKD (Fig. 1D), and its expression was more pronounced in the kidneys of CKD patients. We further investigated Golgi integrity by immunofluorescence staining for the Golgi marker GM130. Compared with control kidneys, kidneys from patients with renal stones exhibited altered Golgi morphology with increased dilation and fragmentation of the Golgi apparatus, suggesting that deposition of renal stones can lead to Golgi stress (Fig. 1F).

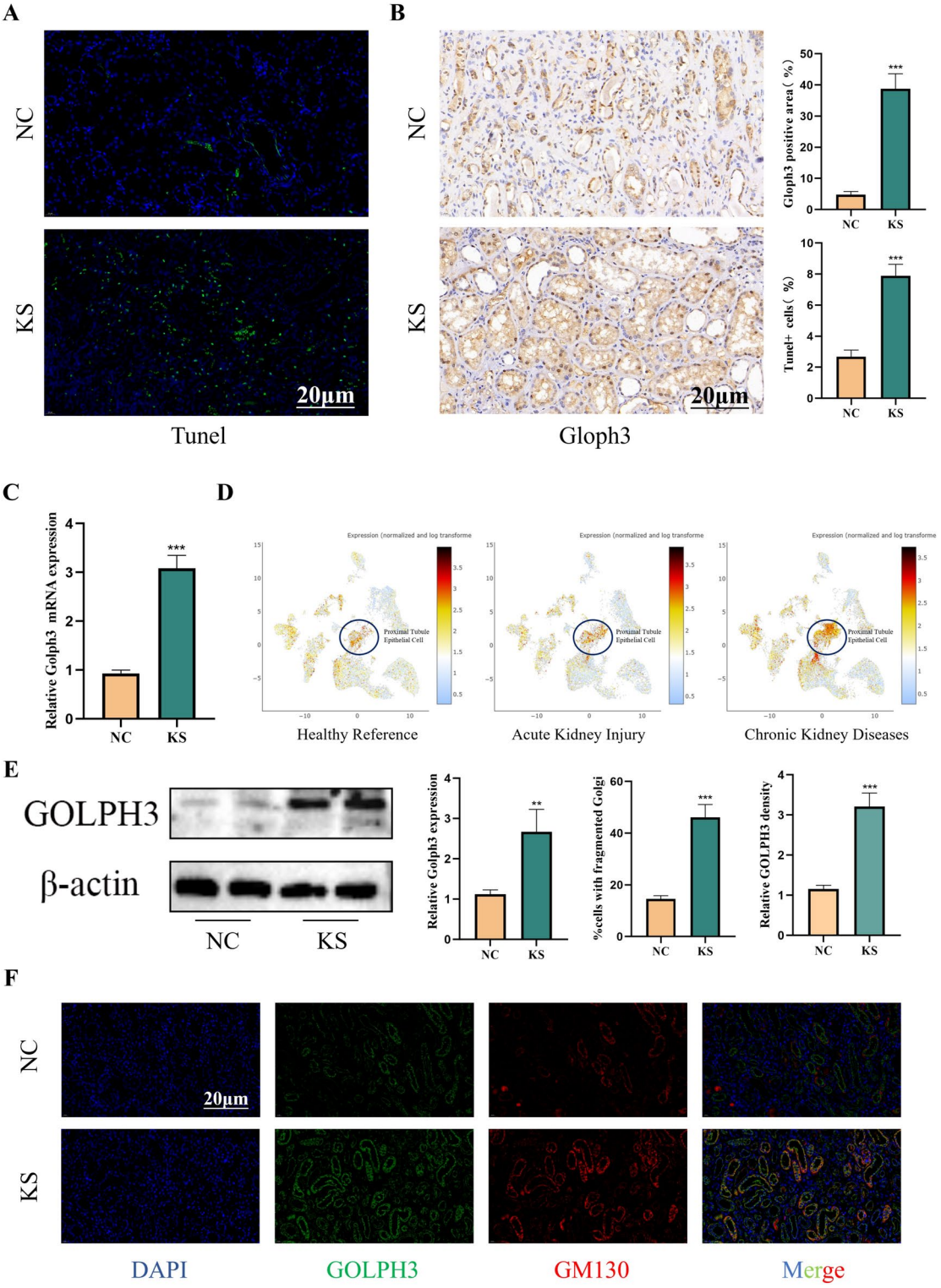

Fig. 1. Up-regulation of GOLPH3 expression in renal tissues of patients with kidney stones (**A**) Representative Tunel staining results of normal renal tissue and renal tissue from patients with renal stones (n = 6). (**B**, **C**, **E**) IHC, qPCR and Western blot analyses of GOLPH3 expression levels in nephrolithiasis patients. (**D**) Online single-cell sequencing database of snRNA-seq validates GOLPH3 expression levels in normal kidneys versus kidneys of AKI and CKD patients. (**F**) Representative images (n = 6) of immunofluorescence staining for GOLPH3 (green) and GM130 (red). Data are the mean ± SEM of at least 3 independent experiments. $^{*}P < 0.05$, $^{***}P < 0.001$ versus NC group.

Glyoxalate-induced stone model promotes renal fibrosis and inflammatory response

To confirm the changes of GOLPH3 in the stone model, we established a mouse kidney stone model by intraperitoneal injection of glyoxalate. 120 mg/kg of glyoxalate per intraperitoneal injection for CaOx crystal deposition for 10 days, the control group received daily intraperitoneal injections of equal amounts of saline. A schematic diagram of mouse modeling is shown in Fig. 2A. As shown in Fig. 2E, kidney stone mice were successfully modeled. Von-Kossa staining showed that intraperitoneal injection of glyoxalate led to the deposition of CaOx crystals in the kidneys of the model group compared with the control group, and HE results showed that the deposited calcium oxalate crystals led to the disorganization of renal tubular cellular arrangement and the infiltration of inflammatory cells. Sirius Red staining and Masson staining showed that collagen fibers were deposited in the kidneys of mice in the stone group, and tunel staining showed increased apoptosis of renal tubular epithelial cells. In addition, calcium oxalate deposition resulted in significantly higher levels of Scr and BUN as well as mRNA expression of KIM-1 and NGAL in the renal stone group, suggesting that calcium oxalate deposition caused severe impairment of renal function in mice compared to the control group (Fig. 2B, C). TNF-α, IL-6, and IL-1β were significantly upregulated in the model group (Fig. 2D). Western blot (Fig. 2F). results were as expected, GOLPH3 expression was elevated in the model group, immunohistochemistry (Fig. 2E) and qPCR (Fig. 2F) experiments were consistent with Western blot.

Deposited calcium oxalate stones cause Golgi stress in renal tubular epithelial cells

As shown in Fig. 3A, compared with control kidneys, kidneys of mice in the stone group exhibited altered Golgi morphology with increased dilation and fragmentation of the Golgi apparatus (Fig. 3A). Western blotting and RT-qPCR analysis showed that the expression of Golgi protein marker GRASP65, ARF4, PI4KIIIβ, and MYO18A in mice in the stone group was significantly upregulated, meanwhile, the mice in the stone group developed EMT characteristics with elevated expression of the mesenchymal cell markers α-SMA, vimentin as well as the fibrogenesis-related marker Collagen I (Fig. 3B, C). These results showed that the deposited calcium oxalate stones cause Golgi stress and EMT progression in renal tubular epithelial cells.

Deposited calcium oxalate stones regulates the PI3K/AKT/mTOR signaling in HK-2 cells

We stimulated HK-2 cells with COM at a concentration of 200 μg/ml to mimic the in vitro environment of kidney stones. We quantified the expression of Golgi protein markers GRASP65, ARF4, PI4KIIIβ, MYO18A, α-SMA, vimentin, and Collagen I by Western blotting. Compared to the control group, the above indicators were increased in the COM-treated HK-2 cells (Fig. 4A), indicating COM treatment causes Golgi stress and EMT progression in HK-2 cells. Immunohistochemistry experiments verified the Golgi morphological changes in the COM group (Fig. 4B). Given the importance of the PI3K/AKT/mTOR pathway in Golph3 activation. We investigated the role of these pathways in the COM treatment group. Western blotting showed that COM treatment can promote phosphorylation of PI3K, AKT, and mTOR in HK2 cells (Fig. 4C), and these results showed that COM can cause activation of the PI3K/AKT/mTOR pathway in HK2 cells.

Inhibition of GOLPH3 reduces apoptosis and inflammatory responses in Golgi stress-mediated HK-2 cells

Next, we investigated whether knockdown GOLPH3 could inhibit apoptosis and inflammatory responses in Golgi stress-mediated HK2 cells. HK-2 cells were transduced with GOLPH3-specific small interfering RNA (siRNA) and control siRNA, and the overexpression efficiency was verified using Western blotting (Fig. 5A). Western blotting and RT-qPCR showed that COM promoted Golgi protein marker GRASP65, ARF4, PI4KIIIβ, MYO18A, and the EMT-characteristic mesenchymal cell markers α-SMA, vimentin and fibrosis marker Collagen I expression were reversed after knocking down GOLPH3 (Fig. 5C, D). Immunohistochemistry experiments verified the Golgi morphological changes (Fig. 5F). In addition, the function of GOLPH3 in COM-treated HK-2 cells apoptosis and inflammation was evaluated. COM groups exhibited significantly increased TNF-α, IL-1β, and IL-6 compared to the control group, the knockdown of GOLPH3 mitigated this effect (Fig. 5B). We also quantified the apoptotic cells with flow cytometry and showed more HK-2 cells underwent apoptosis when treated with COM and this effect was alleviated after knockdown GOLPH3 (Fig. 5E). Western blotting showed that knockdown of GOLPH3 was able to reverse COM-induced PI3K/AKT/mTOR pathway activation (Fig. 5G). Overall, these results suggested that GOLPH3 promotes calcium oxalate-induced renal injury and fibrosis through Golgi stress-mediated apoptosis and inflammatory responses.

Discussion

Calcium oxalate is the most common type of kidney stone and an increasing number of studies have shown that high levels of oxalate in the body is one of the main cause of caox crystal deposition of kidney stones and that proximal and distal renal tubular interactions with oxalate ions are the main cause of renal tubular epithelial cell damage. Normally, calcium oxalate crystals, or oxalates, are excreted in the urine and not deposited in the body. However, due to several genetic and lifestyle problems, calcium oxalate crystals are gradually deposited in the kidneys[28–33]. Long-term deposition of calcium oxalate crystals leads to apoptosis of renal tubular epithelial cells, oxidative stress, and inflammation, resulting in gradual fibrosis of the kidneys and ultimately impaired renal function. Therefore, when treating kidney stones, attention should be paid to the occurrence of renal fibrosis[34–37].

The central role of the Golgi in key cellular processes such as the transport, processing, and sorting of proteins and lipids places it at the forefront of cell research. Several previous studies have shown that the Golgi plays a key role in disease, particularly in neurodegenerative disorders, but the Golgi has rarely been studied in kidney stone disease. GOLPH3 is a highly conserved protein that plays an important role in maintaining the Golgi structure and transporting proteins[38]. Quantitative studies have shown that GOLPH3 can contribute to

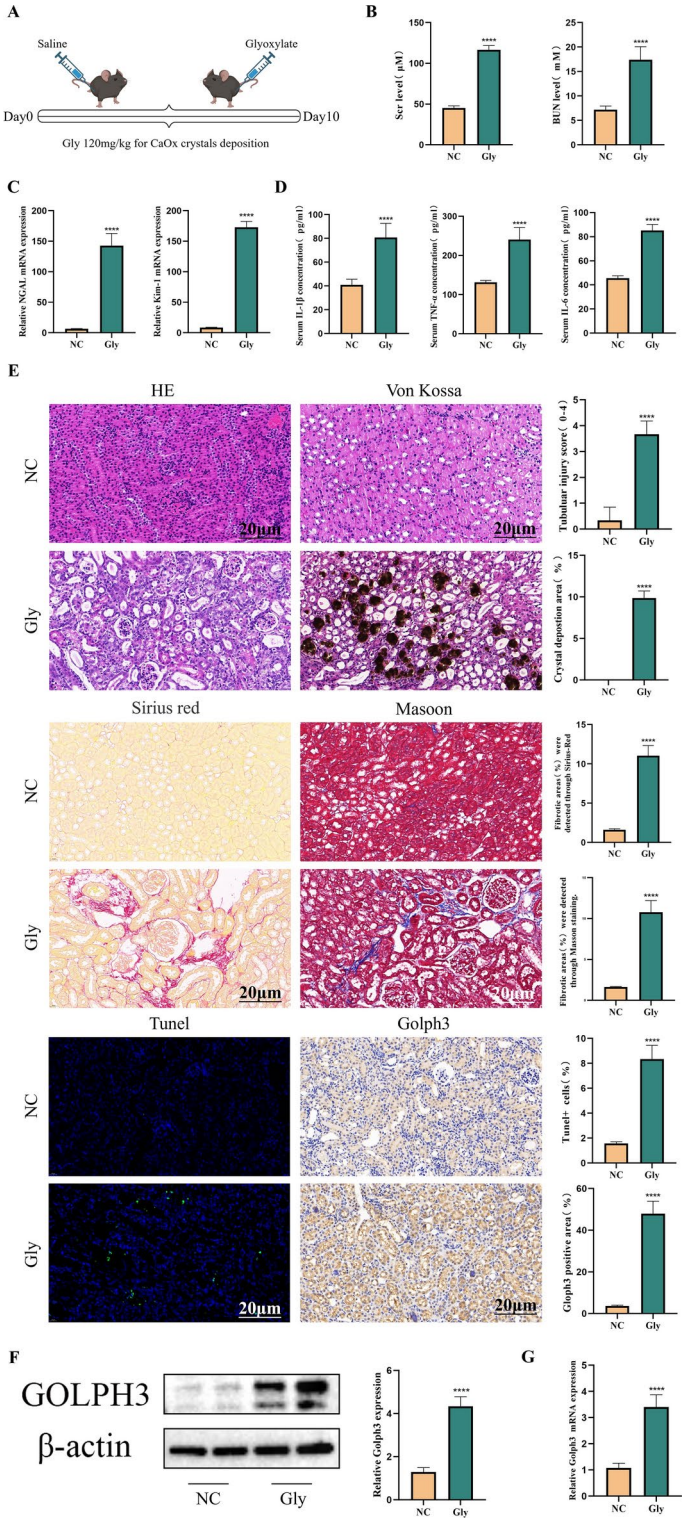

Fig. 2. Glyoxalate-induced stone model promotes renal fibrosis and inflammatory response (**A**) Diagram depicting the experimental design. Measurement of the levels of BUN and Scr in the serum of mice (n = 6). (**C**) mRNA expression of KIM-1 and NGAL in mice kidney tissue. (**D**) Serum levels of pro-inflammatory cytokines TNF-α, IL-1β, and IL-6 were quantified with ELISA. (**E**) Representative images of HE, Von Kossa, Masson, Sirius red, Tunel staining and immunohistochemical staining for GOLPH3 of mouse kidney tissue (n = 6). (**F**, **G**) Western blot and qPCR analyses of GOLPH3 expression levels in mice kidney. Data are the mean ± SEM of at least three independent experiments. $^{****}P < 0.0001$ versus NC group.

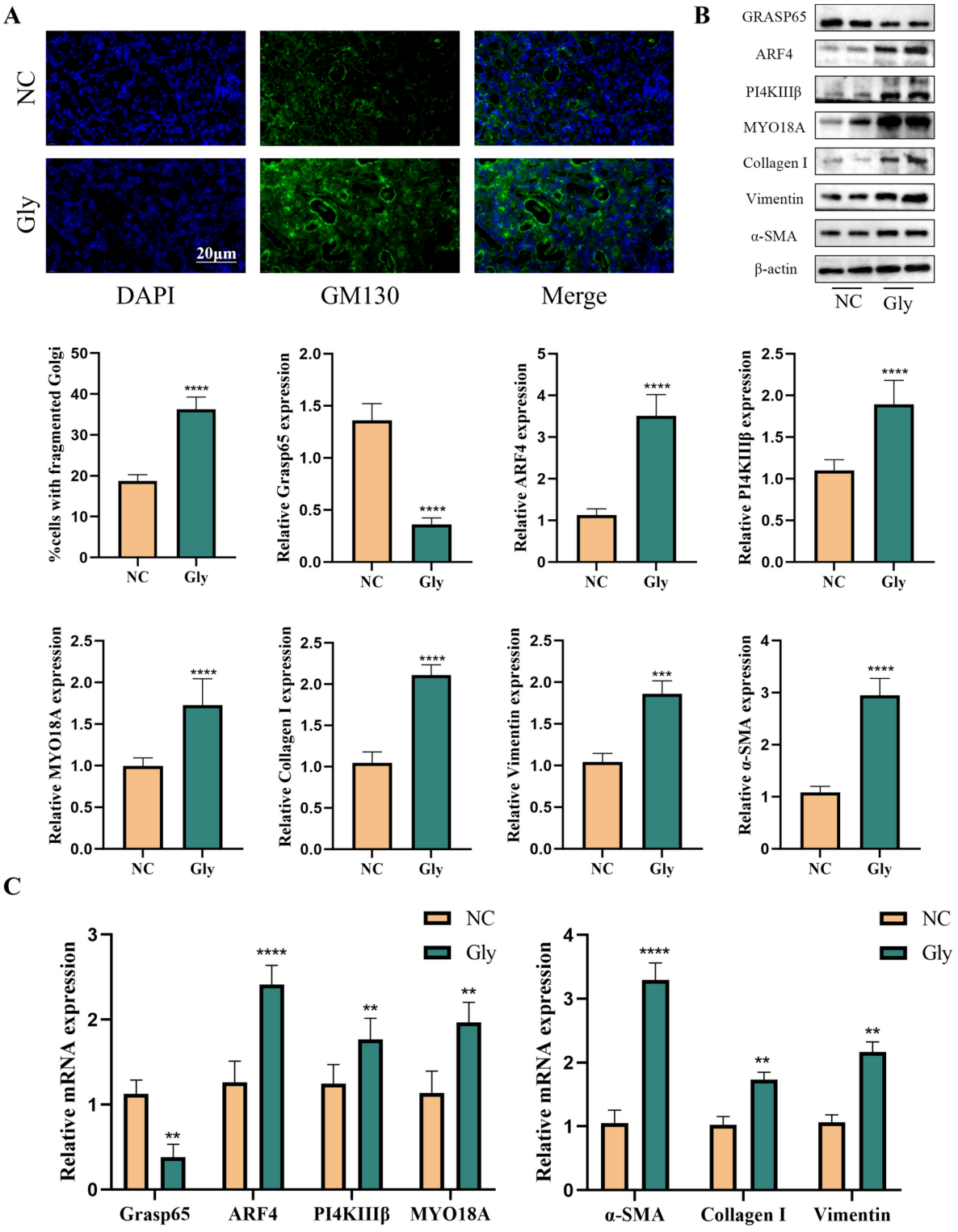

Fig. 3. Deposited calcium oxalate stones cause Golgi stress in renal tubular epithelial cells (**A**) Immunofluorescence staining of Golgi morphological marker GM130 (green) in renal tissue(n = 6). (**B**, **C**) The function and structural proteins of Golgi apparatus (GRASP65, ARF4, PI4KIIIβ and MYO18A) and renal fibrosis related proteins (Collagen I, Vimentin, α-SMA) were detected in renal tissues by Western blots and qRT-PCR analysis. Data are the mean ± SEM of at least three independent experiments. $^{**}P < 0.01$, $^{****}P < 0.0001$ versus NC group.

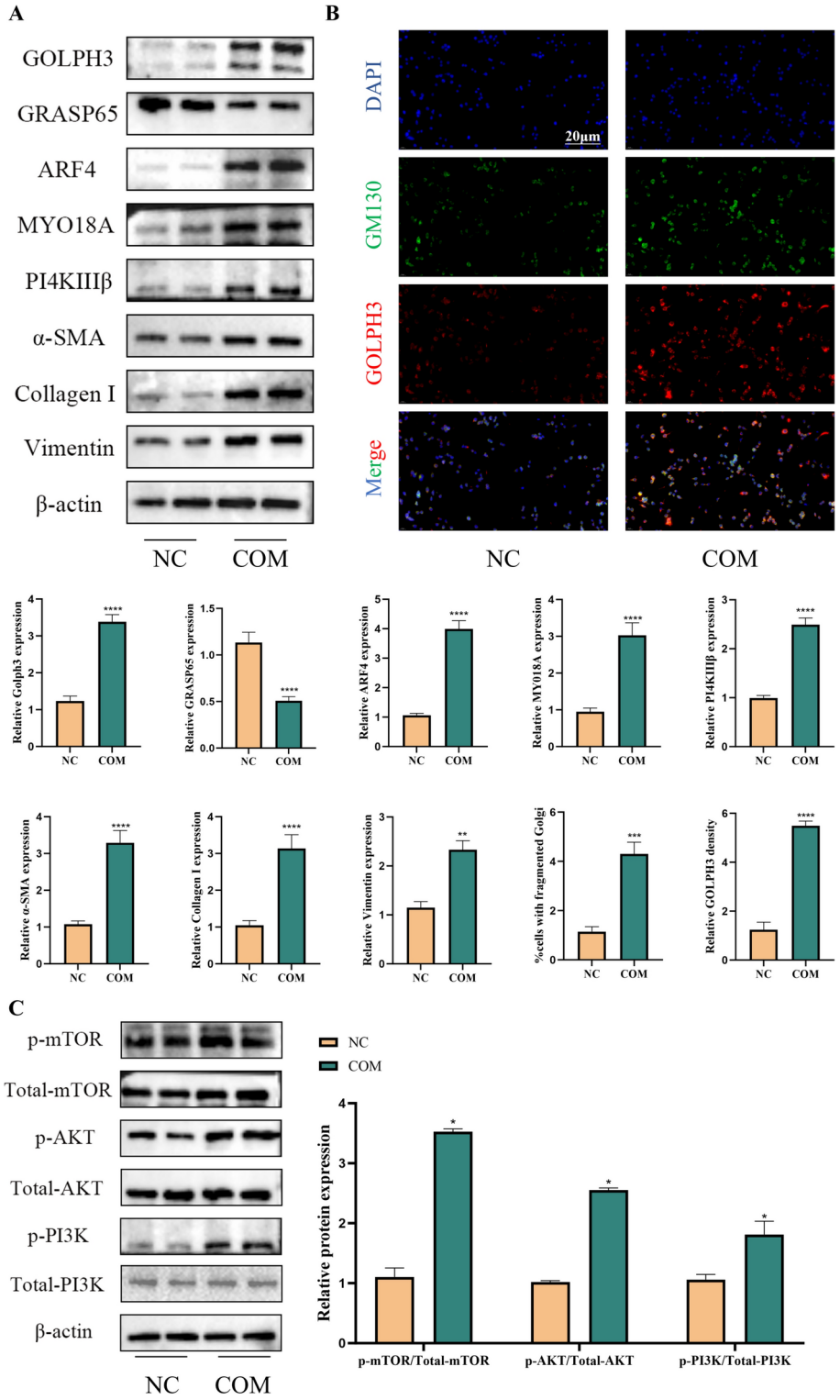

Fig. 4. Deposited calcium oxalate stones regulates the PI3K/AKT/mTOR signaling in HK-2 cells (**A**) Western blots assay was used to detect the expressions of GOLPH3, Golgi structure and functional proteins (GRASP65, ARF4, PI4KIIIβ and MYO18A) and proteins related to renal fibrosis (Collagen I, Vimentin, α-SMA) in HK-2 cells. (**B**) Representative images of immunofluorescence staining of HK-2 cells GOLPH3 (red) and GM130 (green) (**C**) Expressions of PI3K/AKT/mTOR pathway-related proteins in HK-2 cells quantified by Western blotting. Data are the mean ± SEM of at least three independent experiments. $^{*}P<0.05$, $^{**}P<0.01$, $^{***}P<0.001$,$^{****}P<0.0001$ versus NC group.

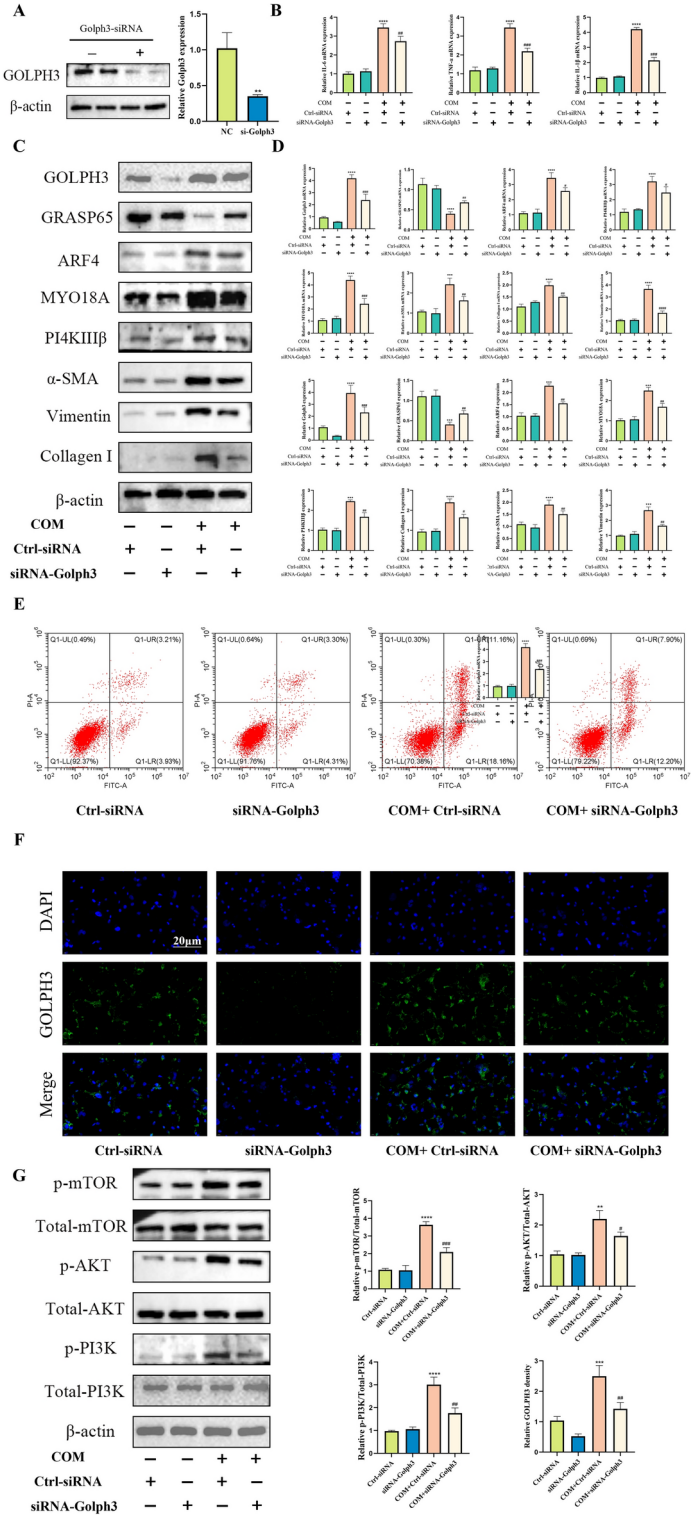

Fig. 5. Inhibition of GOLPH3 reduces apoptosis and inflammatory responses in Golgi stress-mediated HK-2 cells (**A**) Confirmation of siRNA-mediated GOLPH3 knockdown efficiency using immunoblotting in HK-2 cells. (**B**) The levels of TNF-α, IL-6, and IL-1β were determined by qPCR. (**C**, **D**) The expression of GOLPH3, Golgi structural and functional proteins (GRASP65, ARF4, PI4KIIIβ, and MYO18A) and renal fibrosis-related proteins (collagen I, waveform protein, and α-SMA) were detected by Western blotting and qRT-PCR in HK-2 cells in each group. (**E**) After treating HK-2 cells with 200 μg/mL COM for 24 h, the proportion of apoptotic HK-2 cells in each group was assessed by flow cytometry. (**F**) Expression of GOLPH3 in HK-2 cell was detected by immunofluorescence staining, and the percent of positive cells was quantified. (**G**) Western blotting was used to quantify the expression of PI3K/AKT/mTOR pathway-related proteins in HK-2 cells of each group. Data are the mean ± SEM of at least three independent experiments. $^{**}P<0.01$, $^{***}P<0.001$,$^{****}P<0.0001$ versus Ctrl-siRNA group. $^{\#}P<0.01$, $^{\#\#}P<0.01$, $^{\#\#\#}P<0.001$, $^{\#\#\#\#}P<0.0001$ versus Ctrl-siRNA + COM group.

the development of various diseases by regulating downstream molecules such as Rho A, FOXO1, NF-KB, and YB1[39–42]. Wu et al.[43]. found that GOLPH3 promotes glioma progression by facilitating activation of the JAK2-STAT3 pathway, in addition, Jia et al.[44]. reported that GOLPH3 promotes angiogenesis through an epithelial-mesenchymal transition in glioblastoma cells.

However, the development of targeted therapy with GOLPH3 is facing great challenges, because it is an adapter protein with no enzyme activity, which makes it unsuitable as a traditional small molecule inhibitor[17,45,46]. On the contrary, the therapeutic strategy may need to focus on disrupting the protein–protein interaction involving GOLPH3, which introduces additional complexity in drug design and screening. Ensuring selectivity is very important to avoid off-target effect, because GOLPH3 is involved in important cellular processes such as vesicle transport and Golgi maintenance[19,47]. At the same time, the method based on siRNA provides a promising alternative, especially for local kidney diseases, but there are still problems in systemic administration of siRNA due to rapid degradation and off-target effect. Advances in nanoparticle-based drug delivery systems and kidney-targeting ligands may enhance the feasibility of siRNA therapy, although these technologies are still under development[48–53]. Before these strategies are translated into clinical application, pre-clinical research and strict evaluation of long-term safety using kidney-specific drug delivery model are essential.

In this study, by comparing the tissue samples with kidney stones and healthy kidney tissue, we were able to show that the Golgi apparatus was disrupted in the kidney of patients with kidney stones and that secondary necrosis of the renal tubular epithelial cells was increased. Our findings suggest that attention to the role of Golgi stress in kidney stones may provide a potential target for the treatment of this urinary system disease. By searching the public database with single-cell sequencing data, we revealed the increase of GOLPH3 in kidney tissue of patients with AKI and CKD and confirmed the increase of GOLPH3 by establishing an in vitro renal calculi model by treating HK-2 cells with COM. Our other methods, Western blotting, various immunostaining methods, and RT-qPCR, also showed that GOLPH3 expression was consistent with public database queries. By decreasing the expression of GOLPH3 in HK-2 cells, we observed changes in the morphology of the Golgi, functional proteins, fibrosis-associated proteins, pro-inflammatory cytokines, and apoptosis of HK-2 cells that were treated with COM. It is worth mentioning that these conditions have been improved.

Several molecules, such as insulin, glucose, numerous growth factors, and cytokines, have the potential to activate PI3K/AKT/mTOR signaling[54]. Protein kinase B (AKT) plays a critical role in PI3K signaling. In the canonical PI3K/AKT pathway, phosphoinositide-dependent kinase-1 (PDK1) and AKT are brought to the inner surface of the cell membrane through pleckstrin homology (PH) domains. PDK1 then starts AKT1 phosphorylation at Thr308[55]. A crucial downstream branch of AKT is mTORC1. When AKT is phosphorylated, it can phosphorylate mTOR at Ser 2448, which results in the direct activation of mTORC1. Additionally, AKT can phosphorylate tuberous sclerosis complex 2 (TSC2), indirectly activating mTORC1[56]. Furthermore, data indicates that the inhibition of PI3K/AKT/mTOR reduces the severity of acute kidney injury and lung fibrosis induced by lipopolysaccharides[57,58]. We showed by Western blotting experiments that the knockdown of GOLPH3 inhibited the PI3K/AKT/mTOR pathway to alleviate the structure and function of the Golgi apparatus, the physiological status of renal tubular epithelial cells, and the release of inflammatory factors. In conclusion, our findings indicate that the suppression of GOLPH3 expression may attenuate renal inflammation and apoptosis, which are pivotal processes in the pathogenesis of kidney stone formation. While GOLPH3 does not directly inhibit CaOx crystal formation, it plays a pivotal role in maintaining Golgi structure and function, which helps to preserve the cellular environment by reducing stress responses. This, in turn, may reduce factors that promote stone formation and contribute to renal damage. Therefore, studying GOLPH3 and the Golgi apparatus in renal tubular epithelial cells may provide potential targets for the prevention and treatment of kidney stones and renal fibrosis.

Data availability

Data will be made available on request. If anyone would like to request a copy of the data from this study, please contact Baofeng Song at Songbaofeng@whu.edu.com.

Received: 12 November 2024; Accepted: 21 February 2025
Published online: 04 March 2025

References

1. Sorokin, I. et al. Epidemiology of stone disease across the world. *World J. Urol.* **35**(9), 1301–1320 (2017).
2. Albert, A. et al. Expression of heterologous oxalate decarboxylase in HEK293 cells confers protection against oxalate induced oxidative stress as a therapeutic approach for calcium oxalate stone disease. *J. Enzyme Inhib. Med. Chem.* **32**(1), 426–433 (2017).
3. Patel, M. et al. Oxalate induces mitochondrial dysfunction and disrupts redox homeostasis in a human monocyte derived cell line. *Redox. Biol.* **15**, 207–215 (2018).
4. Geraghty, R., Wood, K. & Sayer, J. A. Calcium oxalate crystal deposition in the kidney: Identification, causes and consequences. *Urolithiasis* **48**(5), 377–384 (2020).
5. Joshi, S. & Khan, S. R. Opportunities for future therapeutic interventions for hyperoxaluria: Targeting oxidative stress. *Expert. Opin. Ther. Targets* **23**(5), 379–391 (2019).
6. Khan, S. R. Hyperoxaluria-induced oxidative stress and antioxidants for renal protection. *Urol. Res.* **33**(5), 349–357 (2005).
7. Song, B. F. et al. Overexpression of sirtuin 1 attenuates calcium oxalate-induced kidney injury by promoting macrophage polarization. *Int. Immunopharmacol.* **121**, 110398 (2023).
8. Bucurica, S. et al. Golgi apparatus target proteins in gastroenterological cancers: A comprehensive review of GOLPH3 and GOLGA proteins. *Cells* **12**(14), 1–2 (2023).
9. Buzuk, L. & Hellerschmied, D. Ubiquitin-mediated degradation at the Golgi apparatus. *Front. Mol. Biosci.* **10**, 1197921 (2023).
10. Mohan, A. G. et al. The Golgi apparatus: A Voyage through time, structure, function and implication in neurodegenerative disorders. *Cells* **12**(15), 2–3 (2023).

11. Kim, W. K. et al. Golgi stress response: New insights into the pathogenesis and therapeutic targets of human diseases. *Mol. Cells* **46**(4), 191–199 (2023).
12. Choi, W., Kang, S. & Kim, J. New insights into the role of the Golgi apparatus in the pathogenesis and therapeutics of human diseases. *Arch. Pharm. Res.* **45**(10), 671–692 (2022).
13. Liu, J. et al. The role of the Golgi apparatus in disease (Review). *Int. J. Mol. Med.* **47**(4), 2 (2021).
14. Kwon, Y. et al. Identification of novel pathogenic roles of BLZF1/ATF6 in tumorigenesis of gastrointestinal stromal tumor showing Golgi-localized mutant KIT. *Cell. Death Differ.* **30**(10), 2309–2321 (2023).
15. Vlad, D. B., Dumitrascu, D. I. & Dumitrascu, A. L. Golgi's role in the development of possible new therapies in cancer. *Cells* **12**(11), 3 (2023).
16. Khine, M. N. & Sakurai, K. Golgi-targeting anticancer natural products. *Cancers (Basel)* **15**(7), 1–6 (2023).
17. Sechi, S. et al. Oncogenic roles of GOLPH3 in the physiopathology of cancer. *Int. J. Mol. Sci.* **21**(3), 3–5 (2020).
18. Li, Y. et al. Inhibition of NLRP3 and Golph3 ameliorates diabetes-induced neuroinflammation in vitro and in vivo. *Aging (Albany NY)* **14**(21), 8745–8762 (2022).
19. Buschman, M. D., Xing, M. & Field, S. J. The GOLPH3 pathway regulates Golgi shape and function and is activated by DNA damage. *Front. Neurosci.* **9**, 362 (2015).
20. Rizzo, R. et al. GOLPH3 and oncogenesis: What is the molecular link?. *Tissue Cell.* **49**(2 Pt A), 170–174 (2017).
21. Sechi, S. et al. The multiple cellular functions of the oncoprotein Golgi phosphoprotein 3. *Oncotarget* **6**(6), 3493–3506 (2015).
22. Kiełb, P. et al. Comparative analysis of GOLPH3 expression in lymph node-positive prostate cancer: Immunohistochemistry staining patterns and clinical significance. *Front Oncol* **13**, 1265788 (2023).
23. Huang, A. et al. Golgi phosphoprotein 3 promotes colon cancer cell metastasis through STAT3 and Integrin α3 pathways. *Front. Mol. Biosci.* **9**, 808152 (2022).
24. Yu, T. et al. GOLPH3 inhibition reverses oxaliplatin resistance of colon cancer cells via suppression of PI3K/AKT/mTOR pathway. *Life Sci.* **260**, 118294 (2020).
25. Liu, T. et al. Golgi phosphoprotein 3 promotes ovarian cancer progression and is associated with cisplatin resistance. *J. Cancer Res. Ther.* **18**(2), 488–495 (2022).
26. Hong, Z. S. et al. Tenacissoside H induces apoptosis and inhibits migration of colon cancer cells by downregulating expression of GOLPH3 Gene. *Evid. Based Complement Alternat. Med.* **2020**, 2824984 (2020).
27. Dusabimana, T. et al. GOLPH3 promotes endotoxemia-induced liver and kidney injury through Golgi stress-mediated apoptosis and inflammatory response. *Cell Death Dis.* **14**(7), 458 (2023).
28. Yuan, S. & Larsson, S. C. Coffee and caffeine consumption and risk of kidney stones: A Mendelian randomization study. *Am. J. Kidney Dis.* **79**(1), 9-14.e1 (2022).
29. Qin, Z. et al. Higher triglyceride-glucose index is associated with increased likelihood of kidney stones. *Front. Endocrinol. (Lausanne)* **12**, 774567 (2021).
30. Li, Y. et al. Association between daily sitting time and kidney stones based on the National Health and Nutrition Examination Survey (NHANES) 2007–2016: A cross-sectional study. *Int. J. Surg.* **110**(8), 4624–4632 (2024).
31. Liu, M. et al. Lifestyle factors, serum parameters, metabolic comorbidities, and the risk of kidney stones: A Mendelian randomization study. *Front. Endocrinol. (Lausanne)* **14**, 1240171 (2023).
32. Zhou, Z. et al. Association between alcohol consumption and kidney stones in American adults: 2007–2016 NHANES. *Front. Public Health* **11**, 1156097 (2023).
33. Coe, F. L., Parks, J. H. & Asplin, J. R. The pathogenesis and treatment of kidney stones. *N. Engl. J. Med.* **327**(16), 1141–1152 (1992).
34. Ye, Z. et al. p53 deacetylation alleviates calcium oxalate deposition-induced renal fibrosis by inhibiting ferroptosis. *Biomed. Pharmacother* **164**, 114925 (2023).
35. Xu, Y. et al. Puerarin alleviates apoptosis and inflammation in kidney stone cells via the PI3K/AKT pathway: Network pharmacology and experimental verification. *J. Cell. Mol. Med.* **28**(20), e70180 (2024).
36. Wang, X., Xie, L. & Liu, C. CCR2 antagonist attenuates calcium oxalate-induced kidney oxidative stress and inflammation by regulating macrophage activation. *Exp. Anim.* **73**(2), 211–222 (2024).
37. Su, X. et al. Selenium participates in the formation of kidney stones by alleviating endoplasmic reticulum stress and apoptosis of renal tubular epithelial cells. *Redox Rep.* **29**(1), 2416825 (2024).
38. Wu, C. C. et al. GMx33: A novel family of trans-Golgi proteins identified by proteomics. *Traffic* **1**(12), 963–975 (2000).
39. Zhou, X. et al. GOLPH3 regulates the migration and invasion of glioma cells though RhoA. *Biochem. Biophys. Res. Commun.* **433**(3), 338–344 (2013).
40. Zhang, X. et al. GOLPH3 promotes glioblastoma cell migration and invasion via the mTOR-YB1 pathway in vitro. *Mol. Carcinog.* **54**(11), 1252–1263 (2015).
41. Zeng, Z. et al. Overexpression of GOLPH3 promotes proliferation and tumorigenicity in breast cancer via suppression of the FOXO1 transcription factor. *Clin. Cancer Res.* **18**(15), 4059–4069 (2012).
42. Quesnelle, K. M., Boehm, A. L. & Grandis, J. R. STAT-mediated EGFR signaling in cancer. *J. Cell. Biochem.* **102**(2), 311–319 (2007).
43. Wu, S. et al. GOLPH3 promotes glioma progression via facilitating JAK2-STAT3 pathway activation. *J. Neurooncol.* **139**(2), 269–279 (2018).
44. Jia, J. et al. GOLPH3 promotes vasculogenic mimicry via the epithelial mesenchymal transition in glioblastoma cells. *Turk. Neurosurg.* **33**(5), 722–730 (2023).
45. Kuna, R. S. & Field, S. J. GOLPH3: A Golgi phosphatidylinositol(4)phosphate effector that directs vesicle trafficking and drives cancer. *J. Lipid Res.* **60**(2), 269–275 (2019).
46. Buschman, M. D., Rahajeng, J. & Field, S. J. GOLPH3 links the Golgi, DNA damage, and cancer. *Cancer Res.* **75**(4), 624–627 (2015).
47. Frappaolo, A. et al. GOLPH3 protein controls organ growth by interacting with TOR signaling proteins in Drosophila. *Cell Death Dis.* **13**(11), 1003 (2022).
48. Mottaghitalab, F. et al. Prospects of siRNA applications in regenerative medicine. *Int. J. Pharm.* **524**(1–2), 312–329 (2017).
49. Li, C. et al. Cholesterol-modified DNA nanostructures serve as effective non-viral carriers for delivering siRNA to the kidneys to prevent acute kidney injury. *Small* **20**(30), e2311690 (2024).
50. Huang, X. et al. Targeted drug delivery systems for kidney diseases. *Front. Bioeng. Biotechnol.* **9**, 683247 (2021).
51. Zhou, H. et al. Stimuli-responsive nanotechnology for RNA delivery. *Adv. Sci. (Weinh.)* **10**(36), e2303597 (2023).
52. Nakamura, T. et al. Extrahepatic targeting of lipid nanoparticles in vivo with intracellular targeting for future nanomedicines. *Adv. Drug. Deliv. Rev.* **188**, 114417 (2022).
53. Gomes-da-Silva, L. C., Simões, S. & Moreira, J. N. Challenging the future of siRNA therapeutics against cancer: The crucial role of nanotechnology. *Cell. Mol. Life Sci.* **71**(8), 1417–1438 (2014).
54. Engelman, J. A., Luo, J. & Cantley, L. C. The evolution of phosphatidylinositol 3-kinases as regulators of growth and metabolism. *Nat. Rev. Genet.* **7**(8), 606–619 (2006).
55. Alessi, D. R. et al. Characterization of a 3-phosphoinositide-dependent protein kinase which phosphorylates and activates protein kinase Balpha. *Curr Biol* **7**(4), 261–269 (1997).
56. Manning, B. D. & Toker, A. AKT/PKB signaling: Navigating the network. *Cell* **169**(3), 381–405 (2017).
57. Peng, J. et al. Aspirin alleviates pulmonary fibrosis through PI3K/AKT/mTOR-mediated autophagy pathway. *Exp. Gerontol.* **172**, 112085 (2023).

58. Zhao, Y. et al. Dexmedetomidine protects against lipopolysaccharide-induced acute kidney injury by enhancing autophagy through inhibition of the PI3K/AKT/mTOR pathway. *Front. Pharmacol.* **11**, 128 (2020).

Acknowledgements
This study was supported by a grant from the National Natural Science Foundation of China (82170775, 82100806, 82270802).

Author contributions
BFS.BJL. and ML. wrote the main manuscript text and TR.YR.FC prepared Figs. YSS contributes to the revision of manuscripts.All authors reviewed the manuscript.

Declarations

Competing interests
The authors declare no competing interests.

Additional information
Supplementary Information The online version contains supplementary material available at https://doi.org/10.1038/s41598-025-91638-0.

Correspondence and requests for materials should be addressed to T.R., Y.R. or F.C.

Reprints and permissions information is available at www.nature.com/reprints.

Publisher's note Springer Nature remains neutral with regard to jurisdictional claims in published maps and institutional affiliations.